Synthesis and biochemical evaluation of *O*-acetyl-ADP-ribose and *N*-acetyl analogs†

Lindsay R. Comstock and John M. Denu*

Received 5th July 2007, Accepted 21st August 2007
First published as an Advance Article on the web 4th September 2007
DOI: 10.1039/b710231c

Synthetic routes for the preparation of *O*-acetyl-ADP-ribose and two novel non-hydrolyzable analogs containing an *N*-acetyl are described and shown to interact with the macro domain of histone protein H2A1.1.

Post-translational modifications of histone proteins, specifically acetylation, regulate transcription, DNA synthesis and repair.[1] Dynamic acetylation is controlled by histone acetyltransferases (HATs) and histone deacetylases (HDACs). Evaluation of HDACs is of high interest due to their direct link to cancer and aging.[2] To date, three classes of HDACs have been identified. Class I and II share a conserved catalytic domain and function *via* a zinc-mediated hydrolysis to afford the deacetylated substrate and acetate.[3] Class III HDACs, the sirtuin family of histone–protein deacetylases, play a role in several cellular processes ranging from silencing gene expression, metabolism and apoptosis.[2b,4] Unlike the Class I and II HDACs, the sirtuins require NAD^+ and deacetylation is coupled with the formation of a novel metabolite, *O*-acetyl-ADP-ribose (*O*AADPr) (Fig. 1).[5] Mechanistic investigations support the 2′-*O*-acetyl regioisomer as the enzyme product and that solution equilibrium *via* intra-molecular *trans*-esterification affords a 1 : 1 mixture (at pH 7.5) of the 2′- and 3′-*O*-acetyl regioisomer.[6]

*O*AADPr is hypothesized to be a substrate for other linked enzymatic processes or to serve as an allosteric regulator or second messenger. Early efforts to identify the role of *O*AADPr *in vivo* using microinjections indicated that it caused a delay/block in maturation and cell division in starfish oocytes and blastomeres, respectively.[5b] More recent work has demonstrated that *O*AADPr is capable of interacting with the macro domain of H2A1.1. An atypical histone variant containing an additional 20 kDa domain, macroH2A, has been implicated in transcriptional regulation and proliferation.[7] Additional findings indicate that *O*AADPr may induce the assembly of the yeast Sir complex[8] and modulate cellular responses by regulating the opening of the Ca^{2+}-permeable long transient receptor potential channel 2 (TRPM2).[9]

The identification of additional targets of *O*AADPr is currently restricted by both its inherent instability and the limited quantity available from enzyme derived products.[4b] Hydrolysis occurs at either the acetyl functionality on the ribose sugar or the pyrophosphate linkage by ARH3 (a poly(ADP-ribose) glycohydrolase),[10] Nudix hydrolases,[11] esterases and unidentified metabolizing enzymes.[12] Thus, to effectively evaluate the cellular function of *O*AADPr and to serve as biochemical tools to overcome these limitations, a synthetic pathway to authentic *O*AADPr and two non-hydrolyzable analogs have been developed (Fig. 2). In the design of the non-hydrolyzable analogs, substitution of the *O*-acetyl moiety with an *N*-acetyl is anticipated to greatly stabilize this functionality to both spontaneous and enzyme-dependent hydrolysis, in addition to preventing acyl migration that is typically observed with *O*AADPr. Generation of *N*-acetyl analogs at the 2′- and 3′-positions of the ribose sugar (**2** and **3**) will also prove to be valuable in the identification of the biologically active isomer for each protein target.

Retrosynthetic analysis of *O*AADPr and its *N*-acetyl analogs, indicated that a coupling between AMP and the functionalized ribose sugars would afford the desired products (Fig. 2). Thus, the development of novel synthetic pathways to *O*AADPr and its *N*-acetyl analogs would require the production of three different phosphorylated sugars containing the appropriate substitution at the 2- and 3-positions *via* orthogonal protection strategies. Although it would have been ideal to develop synthetic routes containing common intermediates for introducing substitution on the ribose sugar, literature precedence dictated that different starting materials were necessary.

Department of Biomolecular Chemistry, University of Wisconsin-Madison, Madison, WI, 53706, USA. E-mail: jmdenu@wisc.edu; Fax: +1 (608) 262-5253; Tel: +1 (608)265-1859

† Electronic supplementary information (ESI) available: Complete experimental procedures for all compounds described are provided. Details and results of HPLC stability studies and macroH2A binding experimentals are presented. See DOI: 10.1039/b710231c

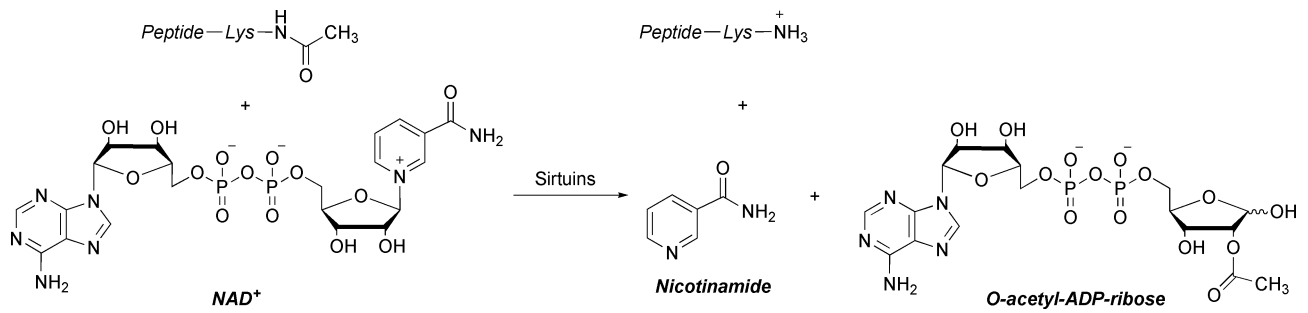

Fig. 1 Sirtuin-mediated deacetylation.

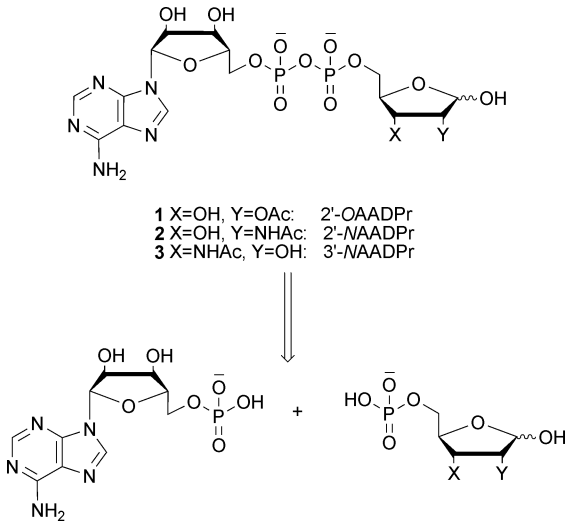

Fig. 2 Retrosynthetic analysis of *O*AADPr and its *N*-acetyl derivatives.

Generation of the functionalized *O*-acetyl ribose is depicted in Scheme 1 and begins with the previously described 5-*O*-benzyl-1,2-*O*-isopropylidene-α-D-xylofuranose (**4**).[13] Inversion of the 3-alcohol was necessary to afford a ribofuranose and accomplished *via* a two-step process involving a PDC oxidation followed by subsequent reduction with $NaBH_4$. Benzylation of the resulting alcohol provided sugar **5** in 52% yield over 3 steps.[13b] Selective protection at the 1-position was initiated with isopropylidene cleavage with Dowex-H^+, followed by a dibutyl stannylene-based benzylation to afford the tri-benzylated ribose, **6**, in 74% yield.[14] Acylation of the resulting alcohol,[15] followed by a selective benzyl deprotection,[16] rendered **7** in 48% yield. Direct phosphorylation using $POCl_3$ in THF,[17] followed by a hydrogenolysis,[18] afforded the TEA salt of sugar **8** (*trans*-esterification mixture of 2′- and 3′-*O*-acetyl regioisomers).

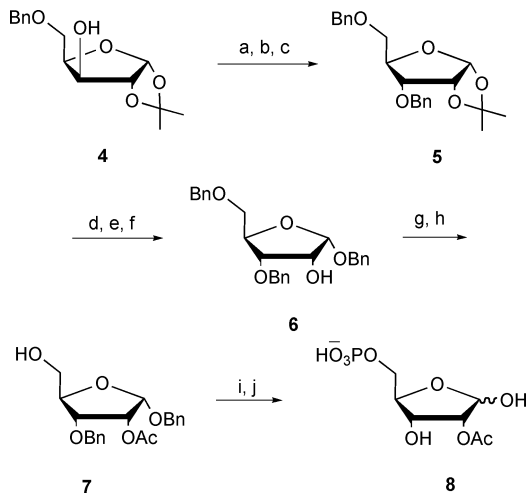

Scheme 1 Synthesis of 2-*O*-acetyl sugar. (a) PDC, AcOH, CH_2Cl_2 (65%); (b) $NaBH_4$, MeOH; (c) BnBr, NaH, DMF (80%, 2 steps); (d) Dowex-H^+, dioxane; (e) Bu_2SnO, MeOH; (f) BnBr, K_2CO_3, DMF (74%, 3 steps); (g) Ac_2O, pyridine (97%); (h) H_2 (50 psi), 10% Pd/C, MeOH–AcOH, 0.08% pyridine (40–50%, 5–15% recovered); (i) $POCl_3$, TEA, THF (85%); (j) H_2 (50 psi), 10% Pd/C, EtOH (88%).

Previous syntheses of nitrogen-bearing ribose analogs substituted at the 2-position have traditionally relied upon azide installation *via* an activated uridine and require subsequent hydrolysis of the uridine base.[19] Due to difficulties in removing the uridine base from the substituted ribose, an alternative synthetic pathway was developed and utilized chemistry previously described by Oppenheimer and Bobek.[20] Instead of directly installing the nitrogen at the desired 2-position of the ribose, the alternative methodology involved its incorporation at the 3-position of a substituted glucofuranose and relocation to the 2-position *via* a $NaIO_4$-mediated oxidative rearrangement.

As depicted in Scheme 2A, conversion of commercially available 1,2:5,6-di-*O*-isopropylidene-α-D-glucofuranose to the azide sugar **9** was accomplished as previously described.[21] Following selective benzylation of the 6-position[22] (**10**), acid hydrolysis of the 1,2-*O*-isopropylidene afforded the requisite sugar for the rearrangement. Oxidation of the 1,2-diol with $NaIO_4$ yielded the corresponding di-aldehyde, which underwent spontaneous ring closure to generate 2-azido ribose sugar **11**.[20] Silyl ether protection of the resulting 1,3-diol afforded **12** as a 1 : 6 mixture of α- and β-anomers in 60% yield.[23] Following reduction of the azide using Staudinger conditions[24] and subsequent acylation of the resulting primary amine,[25] benzyl deprotection was affected using standard hydrogenolysis at 50 psi[18] to afford **13** in 71% yield over three steps. At this stage, the α- and β-anomers were separable using flash chromatography. Direct phosphorylation of either anomer using $POCl_3$[17] of **13** resulted in activated sugar **14** (as the triethylamine salt) for subsequent coupling chemistry in 93% yield.

Installation of the *N*-acetyl at the 3-position of the ribose is depicted in Scheme 2B and bears a resemblance to chemistry developed for substitution at the 2-position. Beginning with **4**, azide installation occurred *via* a S_N2 displacement of the triflate with LiN_3[26] to provide sugar **15** in 38% yield. Upon subjection to Dowex-H^+[19c] to generate the 1,2-diol, subsequent reprotection as the silyl ethers[22] rendered **16** (β anomer only) in a yield of 64%. Following Staudinger reduction of the azide[24] and acylation of the amine,[25] benzyl deprotection produced **17** in 84% yield over three steps.[18] Phosphorylation[17] resulted in the activated sugar **18** (as the triethylamine salt).

To complete the synthesis of *O*AADPr and its *N*-acetyl analogs (**1–3**), the chemistry condensing the adenosine and the functionalized ribose sugar was investigated. Preliminary condensations of sugar phosphates **14** and **18** with AMP failed to yield the anticipated TBS-protected products. It was initially hypothesized that TBS functionalities were interfering sterically with the desired chemistry. Thus, silyl ether deprotection of **14** and **18** was carried out utilizing Dowex-50 (H^+) in high yeilds.[27] The resulting phosphomonoesters **19** and **20** (as the TEA salt), along with *O*-acetyl phosphate **8**, were successfully coupled directly to AMP activated as the diphenyl pyrophosphate (**21**) using procedures established by Michelson (Scheme 3).[28] The resulting products (**1**, **2**, and **3**) were first purified by anion-exchange chromatography (DEAE cellulose) to remove the resulting by-product diadenosine 5′-pyrophosphate (AppA) and followed by preparative HPLC to afford authentic *O*AADPr and its two *N*-acetyl analogs. The yields of the coupling reactions were low (typically 5–20%), but comparable to similar couplings previously carried out.[29]

To validate the installation of an *N*-acetyl as a non-hydrolyzable substitution, the stabilities of both 2′- and 3′-*N*AADPr were

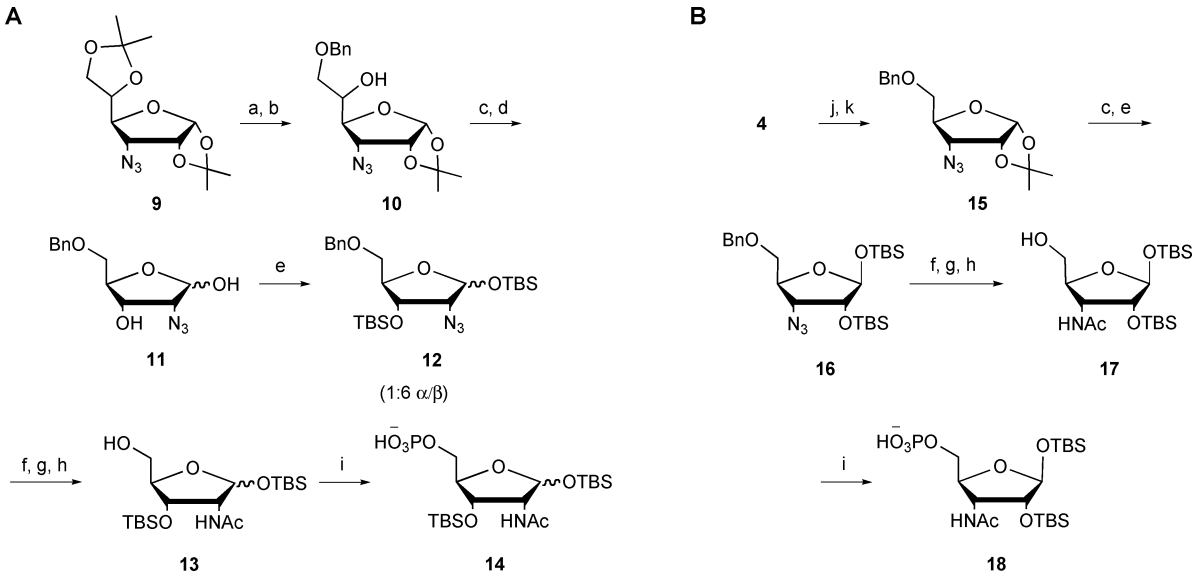

Scheme 2 Synthesis of 2-*N*- and 3-*N*-acetyl sugars. (a) 70% AcOH; (b) Bu_2SnO, toluene, then BnBr and Bu_4NBr (65%, 2 steps); (c) Dowex-H^+, dioxane; (d) $NaIO_4$, $NaHCO_3$ dioxane; (e) TBSCl, imidazole, DMF (**12**: 60%, 3 steps; **16**: 64%, 2 steps); (f) PPh_3, aqueous NH_3, pyridine; (g) Ac_2O, pyridine, CH_2Cl_2; (h) H_2 (50 psi), 10% Pd/C, EtOH (**13**: 71%, 3 steps; **17**: 84%, 3 steps); (i) $POCl_3$, TEA, THF (**14**: 93%; **18**: 90%); (j) Tf_2O, pyridine, CH_2Cl_2 (87%); (k) LiN_3, DMF (44%).

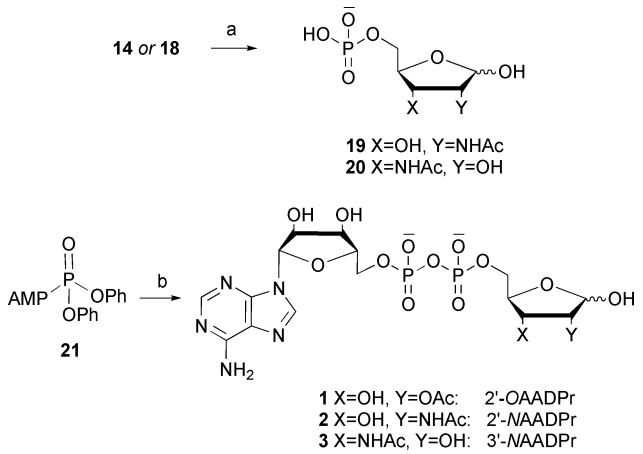

Scheme 3 Phosphate couplings to AMP. (a) Dowex-H^+, ACN (**19**: 97%; **20**: 94%); (b) **8**, **19**, or **20**, DMF, pyridine (5–20%).

evaluated at physiological temperature and pH. Results previously obtained with *O*AADPr indicated that approximately 18% was hydrolyzed spontaneously to ADPr within 3 h.[30] HPLC analysis of both **2** and **3** using the exact conditions indicated negligible decomposition (<1%) over 3 days and confirmed the stability of the acetyl functionality to spontaneous hydrolysis.[31]

Upon completing the synthesis of the *N*-acetyl analogs and confirming their stability, we sought to validate the ability of both 2′- and 3′-*N*AADPr to mimic *O*AADPr. Among several reported protein targets, recent work demonstrated *in vitro* that *O*AADPr binds to macroH2A1.1 histone protein.[7] To establish *N*AADPr binding to macroH2A1.1, isothermal titration calorimetry (ITC) was performed and the titration of ADPr, *O*AADPr, and the *N*-acetyl analogs individually with ligand-free macroH2A1.1 resulted in the binding curves shown in Fig. 3. Resulting dissociation constants and binding enthalpies produced from the binding curves indicate comparable values to those previously determined for ADPr and *O*AADPr (panel A).[7] Both 2′- and 3′-*N*AADPr yielded simililar K_d values (16 *versus* 19 μM, respectively), although there was a small four-fold reduction in values when compared to *O*AADPr (panel B). Similar ΔH values (~13–15 kcal mol^{-1}) among the four suggests a similar mode of binding, likely within the same ligand pocket. Most notable, the nearly identical K_d values of 2′- and 3′-*N*AADPr indicate that macroH2A1.1 does not discriminate between the two regioisomers. Although the *N*AADPr analogs are capable of interacting with macroH2A1.1 in a manner that mimics the natural ligand, further evaluation of the ability of the *N*AADPr analogs to bind competitively with other *O*AADPr-binding proteins/enzymes will be addressed in future studies.

Molecular modeling was performed to evaluate the interactions of macroH2A1.1 with the *N*-acetyl analogs. Utilizing the crystal structure previously determined for ADPr bound to Af1521[32] and macroH2A1.1,[7] both 2′- and 3′-*N*AADPr were modeled into the binding pocket.[33] As shown in Fig. 4, the pocket is capable of accommodating both 2′- (panel A) and 3′-*N*AADPr (panel B) and supports the observed similar dissociation constants for both analogs. Although no obvious structural differences were observed for macroH2A1.1 when modeled with *N*AADPr compared to that obtained with *O*AADPr (data not shown), it is hypothesized that the observed four-fold reduction in binding for both 2′- and 3′-*N*AADPr may be due to minor alterations in the hydrogen bond network.[34] The substitution of the *O*-acetyl moiety with an *N*-acetyl reverses the nature of the hydrogen bond (from an acceptor to a donor).

In summary, the synthetic generation of *O*AADPr and two non-hydrolyzable analogs containing an *N*-acetyl is reported. Subsequent experiments indicated that both 2′- and 3′-*N*AADPr are mimics of *O*AADPr in binding with macroH2A1.1 and

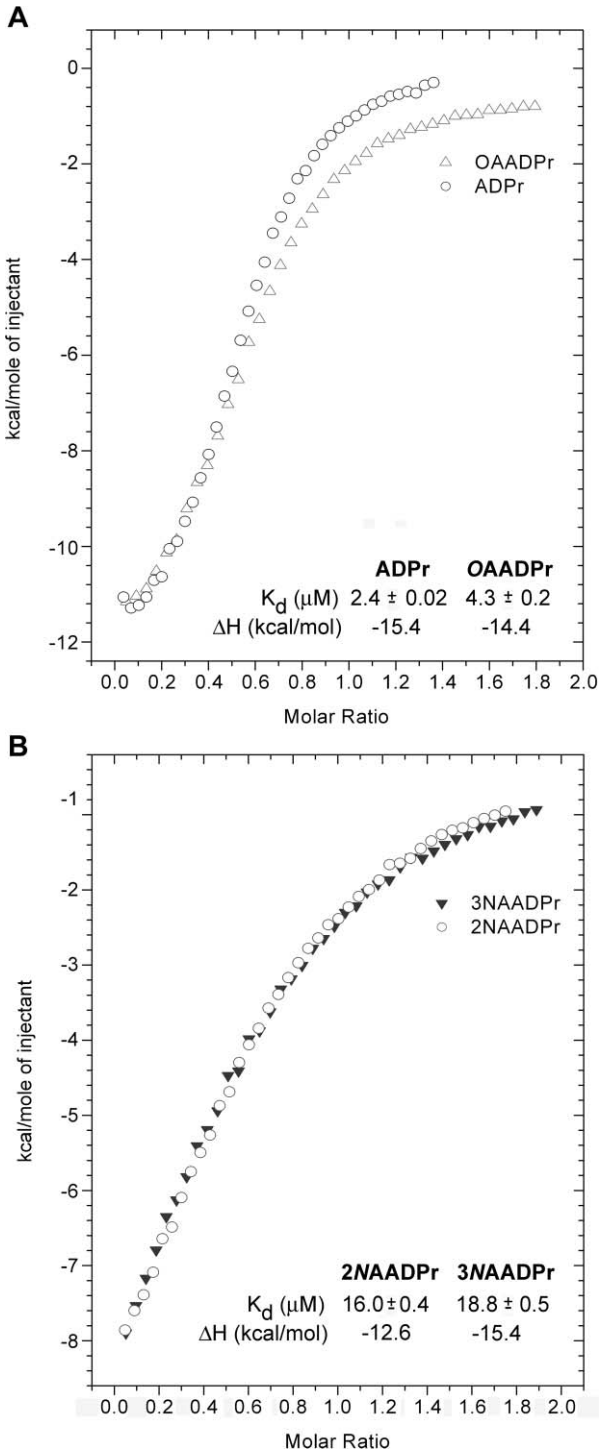

Fig. 3 ITC curves with macroH2A1.1 for (A) ADPr (open circles) and *O*AADPr (open triangles) and (B) 2′-*N*AADPr (open circles) and 3′-*N*AADPr (closed triangles). Experiments were performed at 25 °C in 50 mM KH_2PO_4, pH 6.5 and 1 mM DTT. Values previously obtained for *O*AADPr are 2.6 μM and −17.8 kcal mol^{-1}.[7]

demonstrate that they will be valuable chemical tools for the future evaluation of the physiological role of *O*AADPr. Additionally, these analogs are deemed useful for future studies to uncover unidentified targets of *O*AADPr.

Acknowledgements

This work was supported by grants from the NIH (R01GM065386) and a post-doctoral fellowship (LRC) from the American Heart Association (0625727Z). We thank Dr Alvan Hengge and Dr James Slama for helpful discussions and S. Slauson for work in preparing the *O*-acetyl phosphate sugar. We also thank A. G. Ladurner for providing the macroH2A1.1 plasmid, L. Tong for aiding in the expression of macroH2A1.1 and performing ITC, and B. Smith for performing the SYBYL modeling.

Notes and references

1 S. L. Berger, *Curr. Opin. Genet. Dev.*, 2002, **12**, 142.
2 (*a*) P. A. Marks and M. Dokmanovic, *Expert Opin. Investig. Drugs*, 2005, **14**, 1497; (*b*) S. Hekimi and L. Guarente, *Science*, 2003, **299**, 1351.
3 C. M. Grozinger and S. L. Screiber, *Chem. Biol.*, 2002, **9**, 3.
4 (*a*) J. M. Denu, *Curr. Opin. Chem. Biol.*, 2005, **9**, 431; (*b*) D. Moazed, *Curr. Opin. Cell Biol.*, 2001, **13**, 232.
5 (*a*) M. D. Jackson and J. M. Denu, *J. Biol. Chem.*, 2002, **277**, 18535; (*b*) M. T. Borra, F. J. O'Neill, M. D. Jackson, B. Marshall, E. Verdin, K. R. Foltz and J. M. Denu, *J. Biol. Chem.*, 2002, **277**, 12632.
6 (*a*) A. A. Sauve, I. Celic, J. Avalos, H. Deng, J. D. Boeke and V. L. Schramm, *Biochemistry*, 2001, **40**, 15456; (*b*) B. C. Smith and J. M. Denu, *Biochemistry*, 2006, **45**, 272.
7 G. Kustatscher, M. Hothorn, C. Pugieux, K. Scheffzek and A. G. Ladurner, *Nat. Struct. Mol. Biol.*, 2005, **12**, 624.
8 G. G. Liou, J. C. Tanny, R. G. Kruger, T. Walz and D. Moazed, *Cell*, 2005, **121**, 515.
9 O. Grubisha, L. A. Rafty, C. L. Takanishi, X. Xu, L. Tong, L. A. L. Perraud, A. M. Scharenberg and J. M. Denu, *J. Biol. Chem.*, 2006, **281**, 14057.
10 T. Ono, A. Kasamatsu, S. Oka and J. Moss, *Proc. Natl. Acad. Sci. U. S. A.*, 2006, **103**, 16687.
11 A. S. Mildvan, Z. Xia, H. F. Azurmendi, V. Saraswat, P. M. Legler, M. A. Massiah, S. B. Gabelli, M. A. Bianchet, L. W. Kang and L. M. Amzel, *Arch. Biochem. Biophys.*, 2005, **433**, 129.
12 L. A. Rafty, M. T. Schmidt, A. L. Perraud, A. M. Scharenberg and J. M. Denu, *J. Biol. Chem.*, 2002, **277**, 47114.
13 (*a*) R. D. Marwood, S. Shuto, D. J. Jenkins and B. V. L. Potter, *Chem. Commun.*, 2000, 219; (*b*) P. B. Alper, M. Hendrix, P. Sears and C. H. Wong, *J. Am. Chem. Soc.*, 1998, **120**, 1965.
14 T. L. Su, R. S. Klein and J. J. Fox, *J. Org. Chem.*, 1982, **47**, 1506.
15 J. Ning and F. Kong, *Carbohydr. Res.*, 1997, **300**, 355.
16 B. E. Maryanoff, A. B. Reitz, G. F. Tutwiler, S. J. Benkovic, P. A. Benkovic and S. J. Pilkis, *J. Am. Chem. Soc.*, 1984, **106**, 7851.
17 J. T. Slama, N. Aboul-Ela, D. M. Goli, B. V. Cheesman, A. M. Simmons and M. K. Jacobson, *J. Med. Chem.*, 1995, **38**, 389.
18 C. H. Heathcock and R. Ratcliffe, *J. Am. Chem. Soc.*, 1971, **93**, 1746.
19 (*a*) G. P. Kirschenheuter, Y. Zhai and W. A. Pieken, *Tetrahedron Lett.*, 1994, **35**, 8517; (*b*) J. B. Hobbs and F. Eckstein, *J. Org. Chem.*, 1977, **42**, 714.
20 (*a*) P. R. Sleath, A. L. Handlon and N. J. Oppenheimer, *J. Org. Chem.*, 1991, **56**, 3608; (*b*) M. Bobek and V. Martin, *Tetrahedron Lett.*, 1978, **22**, 1919; (*c*) M. Bobek, *Carbohydr. Res.*, 1979, **70**, 263.
21 M. P. Watterson, L. Pickering, M. D. Smith, S. J. Hudson, P. R. Marsh, J. E. Mordaunt, D. J. Watkin, C. J. Newman and G. W. Fleet, *Tetrahedron: Asymmetry*, 1999, **10**, 1855.
22 (*a*) A. Lubineau and Y. Queneau, *Tetrahedron*, 1989, **45**, 6697; (*b*) R. V. Stick, K. A. Stubbs and A. G. Watts, *Aust. J. Chem.*, 2004, **57**, 779.
23 E. J. Corey and A. Venkateswarlu, *J. Am. Chem. Soc.*, 1972, **94**, 6191.
24 M. R. Webb, G. P. Reid, V. R. Munasinghe and J. E. Corrie, *Biochemistry*, 2004, **43**, 14463.
25 H. B. Mereyala, M. Baseeruddin and S. R. Koduru, *Tetrahedron: Asymmetry*, 2004, **15**, 3457.
26 (*a*) O. Botta, E. Moyroud, C. Lobato and P. Strazewski, *Tetrahedron*, 1998, **54**, 13529; (*b*) A. V. Azhayev, A. M. Ozols, A. S. Bushnev, N. B. Dyatkina, S. V. Kochetova, L. S. Victorova, M. K. Kikhanova, A. A. Krayevsky and B. P. Gottokh, *Nucleic Acids Res.*, 1979, **6**, 625.

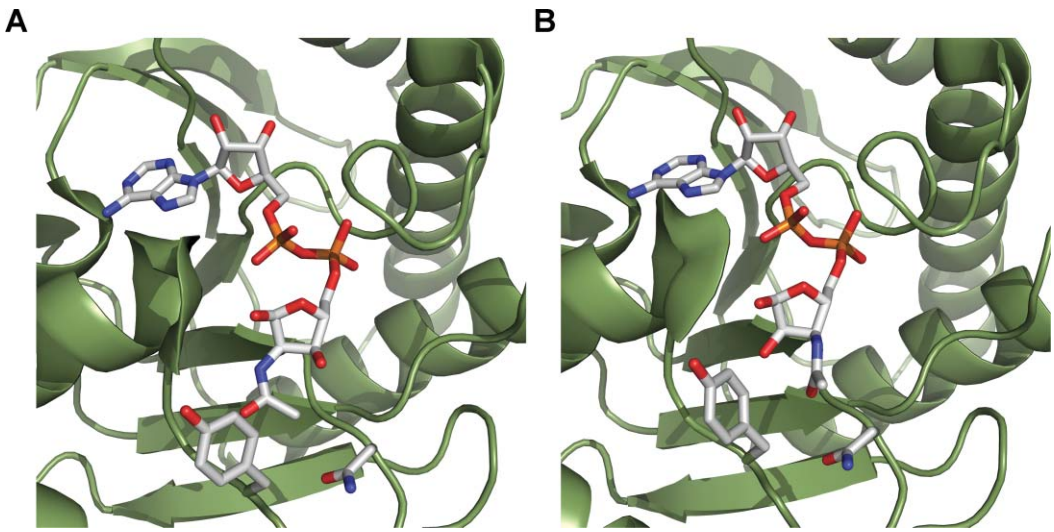

Fig. 4 Molecular modeling of (A) 2′-*N*AADPr and (B) 3′-*N*AADPr with macroH2A1.1 (PDB accession code 2FXK). Color coding: green (macroH2A1.1), grey (carbon), oxygen (red), nitrogen (blue), phosphorus (orange).

27 E. J. Corey, J. W. Ponder and P. Ulrich, *Tetrahedron Lett.*, 1980, **21**, 137.

28 (*a*) A. M. Michelson, *Biochim. Biophys. Acta*, 1964, **91**, 1; (*b*) Q. F. Ma, M. A. Reynolds and G. L. Kenyon, *Bioorg. Chem.*, 1989, **17**, 194. Note: additional methodologies to activate AMP have been described to perform such couplings. See ref. 17 and; D. W. Koh, D. L. Coyle, N. Mehta, S. Ramsinghani, H. Kim, J. T. Slama and M. K. Jacobson, *J. Med. Chem.*, 2003, **46**, 4322.

29 (*a*) S. M. Graham, D. J. Macaya, R. N. Sengupta and K. B. Turner, *Org. Lett.*, 2004, **6**, 233; (*b*) T. Fukui and K. Tanizawa, *Methods Enzymol.*, 1997, **280**, 41.

30 M. T. Borra, F. J. O'Neill, M. D. Jackson, B. Marhsall, E. Verdin, K. R. Foltz and J. M. Denu, *J. Biol. Chem.*, 2002, **277**, 12632.

31 See ESI for experimental details and HPLC traces.

32 G. I. Karras, G. Kustatscher, H. R. Buhecha, M. D. Allen, C. Pugieux, F. Sait, M. Bycroft and A. G. Ladurner, *EMBO J.*, 2005, **24**, 1911.

33 The structure of macroH2A1.1 was not co-crystallized with *O*AADPr. Thus, the crystal structure of ADPr bound to the Af1521 macro domain (PDB accession code 2BFQ) was overlayed with macroH2A1.1 (carbon backbone was matched based upon homology) and the resulting structure of ADPr was utilized as a starting point for modeling the *N*-acetyl analogs into macroH2A1.1. The structure of ADPr was modified in SYBYL, torsionally constrained about the new bonds, and energies minimized across the new structure. PyMol was utilized to produce the images in Fig. 4.

34 Previous studies of the Af1521 macro domain bound to ADPr indicated that mutation of Asn 34 to Ala reduced binding affinity three-fold. See ref. 32.